Published in final edited form as:
AIDS. 2010 February 20; 24(4): 583–592. doi:10.1097/QAD.0b013e3283353c9e.

A Genome-wide Association Study of Carotid Atherosclerosis in HIV-infected Men

Sadeep Shrestha[1,*], **Marguerite M D Irvin**[1], **Kent D Taylor**[2], **Howard W Wiener**[1], **Nicholas M. Pajewski**[3], **Talin Haritunians**[2], **Joseph A. C Delaney**[4], **Morris Schambelan**[5], **Joseph F. Polak**[6], **Donna K Arnett**[1], **Yii-Der Ida Chen**[7], and **Carl Grunfeld**[5]

[1] Department of Epidemiology, School of Public Health, University of Alabama at Birmingham

[2] Pediatrics, School of Medicine, University of California Los Angeles

[3] Department of Biostatistics, School of Public Health, University of Alabama at Birmingham

[4] Department of Biostatistics, University of Washington, Seattle

[5] University of California, San Francisco and Veterans Affairs Medical Center, San Francisco

[6] Tufts Medical Center, Boston

[7] Medical Genetics Institute, Cedars-Sinai Medical Center, University of California Los Angeles

Abstract

Background—The role of host genetics in the development of subclinical atherosclerosis in the context of HIV infected persons who are being treated with highly active antiretroviral therapy (HAART) is not well understood.

Methods—The present genome-wide association study (GWAS) is based on 177 HIV-positive Caucasian males receiving HAART who participated in the Fat Redistribution and Metabolic Change in HIV Infection (FRAM) Study. Common and internal carotid intima-media thicknesses (cIMT) measured by B-mode ultrasound were used as a subclinical measure of atherosclerosis. Single nucleotide polymorphisms (SNPs) were assayed using the Illumina HumanCNV370-quad beadchip. Copy Number Variants (CNV) were inferred using a hidden Markov Model (PennCNV). Regression analyses were used to assess the association of common and internal cIMT with individual SNPs and CNVs, adjusting for age, duration of antiretroviral treatment, and principal components to account for potential population stratification.

Results—Two SNPs in tight linkage disequilibrium, *rs2229116* (a missense, nonsynonymous polymorphism (IIe to Val)) and *rs7177922*, located in the Ryanodine receptor (*RYR3*) gene on chromosome 15 were significantly associated with common cIMT (p-value<1.61×10^{-7}). The *RYR* gene family has been known to play a role in the etiology of cardiovascular disease and has been shown to be regulated by HIV TAT protein.

Conclusions—These results suggest that in the context of HIV infection and HAART, a functional SNP in a biologically plausible candidate gene, *RYR3,* is associated with increased common carotid IMT, which is a surrogate for atherosclerosis.

Keywords

HIV; HAART; atherosclerosis; GWAS; intima-media thickness

[*]Corresponding Author: Sadeep Shrestha, Department of Epidemiology, University of Alabama at Birmingham, 1665 University Blvd, RPHB Room 217L, Birmingham, Alabama 35294-0022, Phone: (205) 934 6459; Fax: (205) 934 8665, sshresth@uab.edu.

Introduction

With increasing effectiveness of highly active antiretroviral therapy (HAART), atherosclerotic vascular disease is emerging as an important complication in HIV [1–3]. HIV infection itself and antiretroviral drugs are associated with dyslipidemia (decreased HDL and increased VLDL cholesterol) and diabetes, which are known to contribute to atherosclerosis [4]. Smoking is increased in populations with HIV infection. However, atherosclerosis is still increased in those with HIV infection even after adjusting for traditional risk factors [5–7]. We have previously reported that HIV-infected patients in this age group have greater common carotid IMT compared with age- and sex-matched control subjects [5]. After multivariable adjustment, HIV infection was associated with 0.033 mm greater in IMT, which can be compared to 0.020 mm for smoking and 0.026 mm for diabetes.

The factors contributing to the independent increase of atherosclerosis in HIV infection have not been fully delineated. Infection with HIV and treatment with antiretroviral drugs have been associated with an increase in systemic inflammation, reduced flow-mediated arterial dilation, and damage to the vascular endothelium which contribute to the development of atherosclerosis [8–11]. Some of the ART drugs used alone or in combination, are associated with serious metabolic abnormalities such as lipoatrophy and dyslipidemia [12,13]. However, in a previous study of FRAM patients that included patients from the present study, while HIV infection was associated with greater IMT after multivariable adjustment for traditional risk factors, no substantial associations of any antiretroviral drugs or classes were found with greater IMT [5]. Genetic susceptibility may contribute to atherosclerosis in HIV infection. Genetic variation accounts for 20–95% of the variation in drug disposition, drug clearance, and duration of action [14]. There are multiple genes involved in the metabolism and transport of drugs that make up the HAART regimen. Variation in expression or activity of such proteins derived from these genes may also relate to the risk for complications, including atherosclerosis, from the use of HAART.

Subclinical atherosclerosis assessed non-invasively using B-mode ultrasound is commonly used in cardiovascular epidemiology studies. The use of a subclinical indicator of atherosclerosis has advantages over evaluating clinical events for several reasons. First, HIV-infected cohorts with a sufficient number of CV events are not available for powerful genome-wide association studies (GWAS). Second, for most clinical CV events, atherosclerotic lesions are a necessary and specific prerequisite, with their presence being predictive of future clinical events [15,16]. In the absence of direct evaluation of anatomically defined lesions, measurement of a correlating phenotype, such as intima-medial thickness (IMT), provides information that is appropriate for genetic studies. Third, clinical CV events are more “genetically removed,” complex, and multi-factorial than intermediate phenotypes defined anatomically and reproducibly measured. Finally, genetic variation in the general population contributes to variation of carotid IMT (cIMT). Derived from large epidemiologic studies, estimates of heritability indicate that 35 to 86% of the variation in cIMT is attributable to shared familial factors [17,18].

In HIV-negative populations, cIMT has been firmly established as a subclinical measure of atherosclerosis and a predictor of incident clinical CV disease, including myocardial infarction and stroke [15,19,20]. Several studies have found that IMT measured in the in the bulb region of the common carotid artery where it branches off into the internal carotid artery, are higher in HIV-positive patients than in HIV-negative controls [5–7]. IMTs are consistently higher in HIV-positive patients than in HIV-negative controls, and increased IMT occurs earlier in HIV-infected patients during treatment than in untreated patients or in the general population [6,21,22]. Despite advances in our understanding of the metabolic

etiology of atherosclerosis in the context of HIV/HAART, studies to date examining genes predicting the atherogenic response to HIV infection/HAART have been limited.

The biological impact of HIV infection and antiretroviral therapy on the development of subclinical atherosclerosis is incompletely understood. There have been only a few candidate genes studied in relation to atherosclerosis in HIV-infected patients [23–26]. To address the need for more comprehensive knowledge and to examine the genetic basis of atherosclerosis, we performed a GWAS involving common and internal cIMTs as intermediate phenotypes in a treated, HIV-infected population.

Study Population

The present study is nested within the Fat Redistribution and Metabolic Change in HIV Infection (FRAM) Study. The recruitment procedure and an overview of the FRAM study have been described elsewhere [27]. Briefly, FRAM was funded by the National Institutes of Health as a cross-sectional study with enrollment of 1,183 HIV-infected persons (825 men, 350 women, and eight transgendered persons) and 297 controls from 16 participating HIV or infectious disease clinics or cohorts. The study participants were enrolled between June 2000 and September 2002. FRAM was initiated to examine the prevalence and correlates of changes in fat distribution, insulin resistance, and dyslipidemia in a geographically and ethnically diverse US population of HIV-infected men and women along with a comparison group of controls. All subjects completed standardized questionnaires used to assess demographics, physical activity and related CV risk behaviors. Also laboratory reports of fasting blood and urine, and detailed medication use including antiretroviral therapy was recorded (as confirmed by medical records [27]; 97% received some form of ART, and 94% received HAART) [5].

The second examination, conducted approximately 5 years later, added carotid IMT measurements to evaluate preclinical atherosclerosis. At this time, participants were phenotyped for all measures collected during the baseline examination. All variables analyzed in this study are from the second visit. Of the 581 HIV+ participants in the follow-up visits, 538 had common or internal cIMT measurements of whom >97% had been on antiretroviral therapy and >94% had been on HAART. To reduce heterogeneity, only male Caucasians with DNA samples (n=177) were included in this study.

Common and Internal Carotid IMT (cIMT)

Standardized IMT measurement protocols and techniques have been previously described [5,15]. Briefly, cIMT measures were obtained by certified ultrasonographers using B-mode ultrasound of the right and left, near and far walls of the common and internal carotid arteries along with the bulb region. Images were analyzed at the Ultrasound Reading Center. One longitudinal lateral view of the distal 10 mm of each common carotid artery and 3 longitudinal views in different imaging planes (anterior, lateral, and posterior) of the each internal carotid artery were obtained. The IMT protocol was also used to capture frozen gray-scale images and cine loops from both carotid arteries on both sides. The common carotid artery is measured with better precision than the internal. The maximal wall thickness of the common carotid artery was determined as the mean of the maximum IMT of the near and far walls of the right and left sides; available measurements from one to four wall locations. The maximal IMT of the internal carotid artery was determined similarly and included the bulb region; measurement sites ranged from one to 12 locations. Two readers measured cIMT due to a staff change and both readers measured both cIMT for 24 of the study participants. The correlation of these 24 measurements was 0.64 and 0.70 for common and internal cIMT, respectively. In the case of such duplicate observations, one cIMT

measurement for each of common and internal carotid cIMT, respectively were chosen at random using the ranuni function in SAS to include in the current analysis.

Genotyping methods

Blood samples were collected during the study visits and consent was specifically obtained for future genetic analyses. DNA was extracted using a Qiagen kit (Qiagen, Valencia, CA) and stored at −70° C. Genotyping was accomplished by use of the Illumina HumanCNV370-quad beadchip (Illumina, San Diego, CA) which probed over 370,000 markers with the Infinium Assay. The HumanCNV370 beadchip includes more than 318,000 tag single nucleotide polymorphism (SNP) markers from the International HapMap Project Phase I and II data, approximately 52,000 markers covering detection of 14,000 copy number variants (CNVs), and 5000 SNPs in the major histocompatibility complex (MHC) region.

Population Sub-structure

The presence of population substructure can be an important confounder in genetic association studies. To detect variability components even within the Caucasian population in the study samples [28], principal components analysis (PCA) implemented in the Eigenstrat software [29] was performed. The PCA technique effectively decomposes the variability present in high-dimensional data sets into lower dimensions to exclude non-homogenous populations. The principle components were derived using genotype data consisting of 337,301 SNPs. As determined by the clustering of the first principal component of the genotypes (data not shown), 5 individuals appeared to have distinct ancestry and seemed to be outliers relative to the rest of the study participants. Using the EIGENSTRAT method in the remaining 172 samples [29], the first PC accounted for 1.27% of genetic variation within our European American population. Subsequent association tests included this component as a covariate in order to control for latent population stratification for common cIMT (n=168) and internal cIMT (n=165) association analyses.

Analysis

Individual SNPs with more than 3% missing data or with low minor allele frequencies (MAF <5%) were removed from the analyses. Using the PLINK software [30], a quantitative trait analysis of the common and internal cIMT was performed using a linear regression model with adjustment for age, duration of HAART in years and the first principal component of the genetic covariance (in the univariate analyses, $CD4^+$ and log(viral-load) were not significantly associated, and were therefore not included in our final analyses). Significance of association was determined by using an allele count χ^2 test with 1 degree of freedom (d.f.) test. Significance levels were adjusted for multiple correction using the *Bonferroni* approach; the levels using both the total number of tests and the effective number of independent tests [31] were considered. Deviations from the expected test statistic null distribution were assessed through quantile-quantile (Q-Q) plots. Two measures of potential inflation of the test statistic were examined: the slope of a line fit to the lower 90% of the distribution ($\lambda_{inflation}$), and the median of the chi-squared statistics for the associations of the included SNPs. In the absence of inflation, $\lambda_{inflation}$ should be 1, and the median of the 2 d.f. chi-squared statistics should be 1.386.

CNVs were characterized with the PennCNV algorithm [32], which takes into consideration the total signal intensity and allelic intensity ratio at each SNP marker, the distance between neighboring SNPs and the allele frequency of each SNP through a Hidden Markov Model. We removed 8 samples based on the previously used criteria for default quality control

threshold recommended by PennCNV: standard deviation for autosomal log R ratio > 0.28, a median B allele frequency of > 0.55 or < 0.45 or a B allele frequency drift of > 0.002 [33]. Copy number calls were required to span at least 10 probes, which has been shown to control false positive calls at a rate lower than 1% [32,34]. CNV calls determined by PennCNV were analyzed by PLINK software. Since PLINK does not allow direct covariate adjustment for CNV analyses, the log cIMT residuals (after adjustment for age, duration of HAART and the first PC values) were used as the outcome variables for both phenotypes. Association analysis was performed for each CNV by combining all the regions that contained each SNP individually. Empirical p-values were calculated using an adaptive permutation approach implemented in PLINK. In order to define regions for association testing of CNVs, merging of CNVs across samples was performed by identifying the common overlapping CNV region for each set of CNVs based on each SNP.

The UCSC Genome Browser was used to locate genes within 250kb upstream or downstream of SNPs that were significantly associated with our phenotypes or located within a CNV region [35]. The Gene Sorter program was then used to identify expression patterns, homology and other information on groups of the identified genes that can be related in many ways [36].

Results

The mean age of our HIV+ population was 49.2 (standard deviation (s.d.) ±9.1) years (range 28–77); they had been in HAART therapy for 6.28 (s.d. ±2.61) years (range 0–10.9). The average common and internal cIMTs were 0.87 (s.d. ±0.17) mm (range 0.57–1.68) and 1.21 (s.d. ±0.49) mm (range 0.50–3.15), respectively.

The GWAS results were based on 311,194 SNPs (6549 with >3% missing data, 6936 monomorphic, 11,317 with <5% minor allele frequency and 1305 with a Hardy-Weinberg equilibrium (HWE) p-value<0.001 were removed) for cIMT and 310,912 SNPs (6351 with >3% missing data, 6941 monomorphic, 11,774 with <5% minor allele frequency and 1305 with HWE p-value<0.001 were removed) for the internal IMT. Allelic association analyses were performed to identify loci associated with common and internal cIMT. Manhattan plots of the association p-values for the two phenotypes are shown in Figures 1a and 1b. As shown in Figure 2, the observed p values did not greatly differ from the expected values over a wide range of values of $[-\mathrm{Log}_{10}(p)]$, from 0 to 4 for common cIMT (Figure 2a) and from 0 to 5 for internal cIMT (Figure 2b). We did not observe any evidence for bias in the test statistics as the Type 1 error rate ($\lambda_{\mathrm{inflation}} = 1.01$) was not inflated and the median of our 2 d.f. chi-squared statistics was 1.379 for common cIMT (Figure 2a), thus uncorrected statistics are presented throughout this paper. Four SNPs had an observed p-value $1-\log_{10}$ greater and 2 had $2-\log_{10}$ greater than the expected p-values for common cIMT association, suggesting that they are likely true genetic variants.

Results for the strongest signals (p-value$<1.5\times10^{-5}$) are shown in Table 1 for the two phenotypes. Two SNPs, *rs2229116* and *rs7177922* (in strong LD, $r^2=0.97$), located in the Ryanodine receptor (*RYR3*) gene were significantly associated (p-value$<1.61\times10^{-7}$) with common cIMT after *Bonferroni* adjustments and effective number of tests. A third SNP in *RYR3* (*rs2291734*, $r^2=0.64$ with *rs222916*) may also be associated with common cIMT (p-value$<2.82\times10^{-6}$). A weaker association was seen with Ryanodine receptor gene *RYR2* (rs12046077, pvalue $< 1.40\times10^{-5}$).

With the implemented quality control-criteria for CNVs, 1565 CNVs (180 double deletions, 649 single deletions, 674 individual insertion and 62 double insertions) were characterized for 164 patients of the study population. The numbers of CNVs ranged from 3 to 28 per

individual. The sizes of the CNVs ranged from 5,739 to 1,131,066 base pairs (bp) and were tagged by 10 to 204 SNPs. While none of the CNVs passed the genome-wide significance threshold of 3.19×10^{-5} for both the common and internal IMT, the most notable CNV was found on chromosome 14 for common cIMT. The common CNV region of 51,632 bp ranging from SNPs *rs11157552* to *rs2141988* (genomic position 21,921,670 to 21,973,302 in chromosome 14) is within the T-cell Receptor Alpha (*TCRA*) gene. There are six individuals with a single deletion in this region; they had the log common cIMT residual measurements of 0.193±0.132 versus −0.007±0.150 mm in those without the deletion (p=0.0005).

Discussion

This report describes the first GWAS evaluating common and internal cIMT, markers of atherosclerosis, among HIV-positive Caucasian men. The results suggest that the gene ryanodine receptor 3 (*RYR3*), located on chromosome 15 is linked to atherosclerosis in HIV-infected individuals. Two SNPs, *rs2229116* and *rs7177922* which are in tight linkage disequilibrium (r^2=0.97) are significantly associated with the common cIMT above the *Bonferroni* correction ($p< 3.4 \times 10^{-8}$ and $p < 2.74 \times 10^{-8}$, respectively). The *rs2229116* SNP is a nonsynonymous polymorphism that has a missense function, as there is a residue change of Ile to Val resulting from the “A” to “G” nucleotide substitution in the sequence. As shown in Figure 3 and Table 1, individuals with the GG genotype have a higher common cIMT than the individuals with AA or AG genotypes. Further, another SNP *rs2291734* (r^2=0.64 with *rs2229116*) in *RYR3* gene, is also associated with greater common cIMT ($p<2.82\times10^{-6}$). These three SNPs lie between recombination hotspots, located within genomic regions 31579227–31580636 and 31718354–31725688 bp in chromosome 15 (Figure 3). Whether the association is due to the direct effects of the missense mutation should be investigated in future studies of the gene in the laboratory. Of note, another SNP, *rs12046077* in the *RYR2* gene (an isoform of *RYR3*) appears to be associated with common cIMT (p-value$< 1.40\times10^{-5}$).

The sequenced *RYR3* cDNA spans 15,564 bp and contains an open reading frame of 14,613 bp. *RYR3,* along with its two isoforms, *RYR1* and *RYR2* [37], are tetramers consisting of 4 identical subunits. The corresponding proteins have a molecular mass around 2200 kDa making these the largest ion-channel proteins that specifically release Ca^{+2} from intracellular stores following transduction of various extracellular stimuli [38]. RYR3 is found in human arterial endothelial cells and plays a role in endothelial vasodilation [39]; endothelial vasodilation is compromised in atherosclerosis. It is of interest that HIV-1 Tat, an important factor in viral pathogenesis, has been shown to cause endothelial dysfunction [40]. HIV-1 Tat can induce rapid loss of endoplasmic reticulum Ca^{+2} through the mediation of *RYR*s [41]. RYR has been shown to be up-regulated in the atherosclerotic aorta of atherosclerosis-prone mice compared to atherosclerosis-resistant mice [42]. In a study of mice on western diet, oxidized LDL induced a dose-dependent rise in intracellular calcium in aortic endothelial cells and increased monocyte chemoattractant protein-1 production. Chemically inhibiting intracellular calcium alleviated the effect of oxidized LDL on monocyte chemoattractant protein-1 production [42]. Though future laboratory studies are needed to determine the functional relationship of these RYR3 SNPS with the pathology of atherosclerosis among ART treated HIV-infected patients, evidence in the literature creates a foundation for a role of RYR calcium signaling in the inflammatory process of atherogenesis in the artery.

Similarly, a deletion of the CNV region within the *TCRA* gene in chromosome 14 suggests an association with common cIMT. *TCRA* encodes one of two polypeptide subunits that make up immunoglobulin-like integral membrane glycoproteins on the receptors of T cells,

which are responsible for recognizing antigens bound to MHC molecules. In one study, genomic region around *TCRA* has been localized for familiar hypertrophic cardiomyopathy [43]. Other studies have shown the presence of T-lymphocytes, mostly bearing alpha/beta TCR, in atherosclerotic lesions [44,45]. T-lymphocytes are a key target of HIV itself.

The present study involves a relatively homogenous population of white men receiving HAART therapy. It is known that HIV and antiretroviral therapy both have a cumulative effect on risk factors for CV diseases, including atherosclerosis [1,4,5]. Most patients in industrialized nations are now treated with antiretroviral drugs. Like many cohorts, more than 94% of the FRAM subjects who had IMT performed had been on HAART and >97% had received antiretroviral drugs. Given these data, we cannot assess whether the genetic associations are unique to HAART. Although there was an adjustment for the differential duration of HAART, the cross-sectional measurements of IMTs is also a limitation of the study. Common cIMT can be measured with greater accuracy than the internal carotid artery [46]. Since, the cIMT measure is reproducible, and valid [47,48], the observed association of SNPs in *RYR3* gene with common cIMT is convincing.

Another limitation with this study is the small sample size. Based on the simulation-based power calculation, assuming a standard deviation of approximately 0.15 units (in log-scale), as for common cIMT, with the sample size of this present study, there is 80% power to detect differences in the log-transformed common cIMT log(cIMT) of at least 0.08 for SNPs with MAF of 10% and at least 0.06 for MAF 25%. But theoretically, there would be no power to detect significant difference considering multiple comparisons. Of note however, the minor allele frequency (MAF) for the strongest result was 18% and the observed difference in log(cIMT) between highest and lowest groups (two homozygotes) was about 0.33, which would theoretically correspond to an additive model difference of 0.17. Thus, the finding from this study, which passes even stringent *Bonferroni* adjustment, suggests a true association and needs to be evaluated further.

Continued research is needed to understand the effects of HIV infection and antiretroviral therapy on CVD risk. Large-scale, long-term longitudinal studies are necessary to resolve the conflicting findings regarding accelerated atherosclerosis in HIV-infected individuals treated with HAART, but such studies may not be feasible. Therefore, further research on the underlying genetic influences may illuminate the molecular mechanisms involved in atherosclerosis within and outside the context of HIV and its treatment. Although the resulting polymorphisms seen in this study need to be validated in larger cohorts within similar and other ethnic populations, these genetic variants should lead to identification of biological pathways for atherosclerosis in the context of HIV/HAART. This information could be used to develop innovative therapeutic or preventive interventions to reduce the burden of atherosclerosis in this high-risk population. While the results from this study are preliminary, they show the potential for identification of atherosclerosis genes, particularly in the context of HIV and HAART treatment.

Acknowledgments

We thank investigators and staff of the Fat Redistribution and Metabolic Change in HIV Infection (FRAM) Study. We would also like to thank the following individuals for their valuable consultation and input: Dr. Hemant K Tiwari with GWAS analyses, Dr. Rebecca Scherzer with FRAM data, Dr. Daniel O'Leary with the IMT data, and Dr. Jerome I Rotter with the study design. The parent study and this sub-study conformed to the procedures for informed consent approved by institutional review boards at all sponsoring organizations and to human-experimentation guidelines set forth by the United States Department of Health and Human Services. The FRAM study was supported by grants from the NIH (R01-DK57508, HL74814, and HL53359, K23 AI66943, and NIH center grants M01-RR00036, RR00051, RR00052, RR00054, RR00083, RR00636, RR00865 and UL1 RR024131) and the Albert L. and Janet A. Schultz Supporting Foundation. The funding agencies had no role in the collection or

analysis of the data. The genotyping efforts were supported by NCRR grant M01-RR00425 (GCRC), DERC grant DK063491, and the Cedars-Sinai Board of Governors Chair in Medical Genetics (JIR).

References

1. Currier JS, Lundgren JD, Carr A, Klein D, Sabin CA, Sax PE, et al. Epidemiological evidence for cardiovascular disease in HIV-infected patients and relationship to highly active antiretroviral therapy. Circulation. 2008; 118:e29–35. [PubMed: 18566319]
2. Martinez E, Larrousse M, Gatell JM. Cardiovascular disease and HIV infection: host, virus, or drugs? Curr Opin Infect Dis. 2009; 22:28–34. [PubMed: 19532078]
3. Grinspoon SK, Grunfeld C, Kotler DP, Currier JS, Lundgren JD, Dube MP, et al. State of the science conference: Initiative to decrease cardiovascular risk and increase quality of care for patients living with HIV/AIDS: executive summary. Circulation. 2008; 118:198–210. [PubMed: 18566320]
4. Grunfeld C, Kotler DP, Arnett DK, Falutz JM, Haffner SM, Hruz P, et al. Contribution of metabolic and anthropometric abnormalities to cardiovascular disease risk factors. Circulation. 2008; 118:e20–28. [PubMed: 18566314]
5. Grunfeld C, Delaney JA, Wanke C, Currier JS, Scherzer R, Biggs ML, et al. Preclinical atherosclerosis due to HIV infection: carotid intima-medial thickness measurements from the FRAM study. Aids. 2009
6. Lorenz MW, Stephan C, Harmjanz A, Staszewski S, Buehler A, Bickel M, et al. Both long-term HIV infection and highly active antiretroviral therapy are independent risk factors for early carotid atherosclerosis. Atherosclerosis. 2008; 196:720–726. [PubMed: 17275008]
7. Hsue PY, Lo JC, Franklin A, Bolger AF, Martin JN, Deeks SG, Waters DD. Progression of atherosclerosis as assessed by carotid intima-media thickness in patients with HIV infection. Circulation. 2004; 109:1603–1608. [PubMed: 15023877]
8. Reingold J, Wanke C, Kotler D, Lewis C, Tracy R, Heymsfield S, et al. Association of HIV infection and HIV/HCV coinfection with C-reactive protein levels: the fat redistribution and metabolic change in HIV infection (FRAM) study. J Acquir Immune Defic Syndr. 2008; 48:142–148. [PubMed: 18344877]
9. Kuller LH, Tracy R, Belloso W, De Wit S, Drummond F, Lane HC, et al. Inflammatory and coagulation biomarkers and mortality in patients with HIV infection. PLoS Med. 2008; 5:e203. [PubMed: 18942885]
10. Stein JH, Klein MA, Bellehumeur JL, McBride PE, Wiebe DA, Otvos JD, Sosman JM. Use of human immunodeficiency virus-1 protease inhibitors is associated with atherogenic lipoprotein changes and endothelial dysfunction. Circulation. 2001; 104:257–262. [PubMed: 11457741]
11. Torriani FJ, Komarow L, Parker RA, Cotter BR, Currier JS, Dube MP, et al. Endothelial function in human immunodeficiency virus-infected antiretroviral-naive subjects before and after starting potent antiretroviral therapy: The ACTG (AIDS Clinical Trials Group) Study 5152s. J Am Coll Cardiol. 2008; 52:569–576. [PubMed: 18687253]
12. Carr A, Samaras K, Thorisdottir A, Kaufmann GR, Chisholm DJ, Cooper DA. Diagnosis, prediction, and natural course of HIV-1 protease-inhibitor-associated lipodystrophy, hyperlipidaemia, and diabetes mellitus: a cohort study. Lancet. 1999; 353:2093–2099. [PubMed: 10382692]
13. Carr A. HIV lipodystrophy: risk factors, pathogenesis, diagnosis and management. Aids. 2003; 17 (Suppl 1):S141–148. [PubMed: 12870540]
14. Kalow W, Tang BK, Endrenyi L. Hypothesis: comparisons of inter- and intra-individual variations can substitute for twin studies in drug research. Pharmacogenetics. 1998; 8:283–289. [PubMed: 9731714]
15. O'Leary DH, Polak JF, Kronmal RA, Manolio TA, Burke GL, Wolfson SKJ. Carotid-artery intima and media thickness as a risk factor for myocardial infarction and stroke in older adults. Cardiovascular Health Study Collaborative Research Group. N Engl J Med. 1999; 340:14–22. [PubMed: 9878640]

16. Hodis HN, Mack WJ, LaBree L, Selzer RH, Liu CR, Liu CH, Azen SP. The role of carotid arterial intima-media thickness in predicting clinical coronary events. Ann Intern Med. 1998; 128:262–269. [PubMed: 9471928]

17. Duggirala R, Gonzalez Villalpando C, O'Leary DH, Stern MP, Blangero J. Genetic basis of variation in carotid artery wall thickness. Stroke. 1996; 27:833–837. [PubMed: 8623101]

18. Fox CS, Polak JF, Chazaro I, Cupples A, Wolf PA, D'Agostino RA, O'Donnell CJ. Genetic and environmental contributions to atherosclerosis phenotypes in men and women: heritability of carotid intima-media thickness in the Framingham Heart Study. Stroke. 2003; 34:397–401. [PubMed: 12574549]

19. Grobbee DE, Bots ML. Carotid artery intima-media thickness as an indicator of generalized atherosclerosis. J Intern Med. 1994; 236:567–573. [PubMed: 7964435]

20. Mack WJ, LaBree L, Liu C, Selzer RH, HNH. Correlations between measures of atherosclerosis change using carotid ultrasonography and coronary angiography. Atherosclerosis. 2000; 150:371–379. [PubMed: 10856529]

21. Mercie P, Thiebaut R, Aurillac-Lavignolle V, Pellegrin JL, Yvorra-Vives MC, Cipriano C, et al. Carotid intima-media thickness is slightly increased over time in HIV-1-infected patients. HIV Med. 2005; 6:380–387. [PubMed: 16268819]

22. Periard D, Cavassini M, Taffe P, Chevalley M, Senn L, Chapuis-Taillard C, et al. High prevalence of peripheral arterial disease in HIV-infected persons. Clin Infect Dis. 2008; 46:761–767. [PubMed: 18230043]

23. Alonso-Villaverde C, Coll B, Parra S, Montero M, Calvo N, Tous M, et al. Atherosclerosis in patients infected with HIV is influenced by a mutant monocyte chemoattractant protein-1 allele. Circulation. 2004; 110:2204–2209. [PubMed: 15466648]

24. Coll B, Alonso-Villaverde C, Parra S, Montero M, Tous M, Joven J, Masana L. The stromal derived factor-1 mutated allele (SDF1-3'A) is associated with a lower incidence of atherosclerosis in HIV-infected patients. Aids. 2005; 19:1877–1883. [PubMed: 16227796]

25. Floris-Moore M, Fayad ZA, Berman JW, Mani V, Schoenbaum EE, Klein RS, et al. Association of HIV viral load with monocyte chemoattractant protein-1 and atherosclerosis burden measured by magnetic resonance imaging. Aids. 2009; 23:941–949. [PubMed: 19318907]

26. Coll B, Alonso-Villaverde C, Joven J. Monocyte chemoattractant protein-1 and atherosclerosis: is there room for an additional biomarker? Clin Chim Acta. 2007; 383:21–29. [PubMed: 17521622]

27. Tien PC, Benson C, Zolopa AR, Sidney S, Osmond D, Grunfeld C. The study of fat redistribution and metabolic change in HIV infection (FRAM): methods, design, and sample characteristics. Am J Epidemiol. 2006; 163:860–869. [PubMed: 16524955]

28. Paschou P, Drineas P, Lewis J, Nievergelt CM, Nickerson DA, Smith JD, et al. Tracing substructure in the European American population with PCA-informative markers. PLoS Genet. 2008; 4:e1000114. [PubMed: 18797516]

29. Price AL, Patterson NJ, Plenge RM, Weinblatt ME, Shadick NA, Reich D. Principal components analysis corrects for stratification in genome-wide association studies. Nat Genet. 2006; 38:904–909. [PubMed: 16862161]

30. Purcell S, Neale B, Todd-Brown K, Thomas L, Ferreira MA, Bender D, et al. PLINK: a tool set for whole-genome association and population-based linkage analyses. Am J Hum Genet. 2007; 81:559–575. [PubMed: 17701901]

31. Gao X, Becker LC, Becker DM, Starmer JD, Province MA. Avoiding the high Bonferroni penalty in genome-wide association studies. Genet Epidemiol. 2009

32. Wang K, Li M, Hadley D, Liu R, Glessner J, Grant S, et al. PennCNV: an integrated hidden Markov model designed for high-resolution copy number variation detection in whole-genome SNP genotyping data. Genome Res. 2007; 17:1665–1674. [PubMed: 17921354]

33. Bucan M, Abrahams BS, Wang K, Glessner JT, Herman EI, Sonnenblick LI, et al. Genome-wide analyses of exonic copy number variants in a family-based study point to novel autism susceptibility genes. PLoS Genet. 2009; 5:e1000536. [PubMed: 19557195]

34. Jakobsson M, Scholz SW, Scheet P, Gibbs JR, VanLiere JM, Fung HC, et al. Genotype, haplotype and copy-number variation in worldwide human populations. Nature. 2008; 451:998–1003. [PubMed: 18288195]

35. Pevsner J. Analysis of genomic DNA with the UCSC genome browser. Methods Mol Biol. 2009; 537:277–301. [PubMed: 19378150]

36. Kent WJ, Hsu F, Karolchik D, Kuhn RM, Clawson H, Trumbower H, Haussler D. Exploring relationships and mining data with the UCSC Gene Sorter. Genome Res. 2005; 15:737–741. [PubMed: 15867434]

37. Sutko JL, Airey JA. Ryanodine receptor Ca2+ release channels: does diversity in form equal diversity in function? Physiol Rev. 1996; 76:1027–1071. [PubMed: 8874493]

38. Leeb T, Brenig B. cDNA cloning and sequencing of the human ryanodine receptor type 3 (RYR3) reveals a novel alternative splice site in the RYR3 gene. FEBS Lett. 1998; 423:367–370. [PubMed: 9515741]

39. Kohler R, Brakemeier S, Kuhn M, Degenhardt C, Buhr H, Pries A, Hoyer J. Expression of ryanodine receptor type 3 and TRP channels in endothelial cells: comparison of in situ and cultured human endothelial cells. Cardiovasc Res. 2001; 51:160–168. [PubMed: 11399258]

40. Paladugu R, Fu W, Conklin BS, Lin PH, Lumsden AB, Yao Q, Chen C. Hiv Tat protein causes endothelial dysfunction in porcine coronary arteries. J Vasc Surg. 2003; 38:549–555. discussion 555–546. [PubMed: 12947275]

41. Norman JP, Perry SW, Reynolds HM, Kiebala M, De Mesy Bentley KL, Trejo M, et al. HIV-1 Tat activates neuronal ryanodine receptors with rapid induction of the unfolded protein response and mitochondrial hyperpolarization. PLoS One. 2008; 3:e3731. [PubMed: 19009018]

42. Yuan Z, Miyoshi T, Bao Y, Sheehan JP, Matsumoto AH, Shi W. Microarray analysis of gene expression in mouse aorta reveals role of the calcium signaling pathway in control of atherosclerosis susceptibility. Am J Physiol Heart Circ Physiol. 2009; 296:H1336–1343. [PubMed: 19304945]

43. Hejtmancik JF, Brink PA, Towbin J, Hill R, Brink L, Tapscott T, et al. Localization of gene for familial hypertrophic cardiomyopathy to chromosome 14q1 in a diverse US population. Circulation. 1991; 83:1592–1597. [PubMed: 2022018]

44. Emeson EE, Robertson AL Jr. T lymphocytes in aortic and coronary intimas. Their potential role in atherogenesis. Am J Pathol. 1988; 130:369–376. [PubMed: 3257650]

45. Kleindienst R, Xu Q, Willeit J, Waldenberger FR, Weimann S, Wick G. Immunology of atherosclerosis. Demonstration of heat shock protein 60 expression and T lymphocytes bearing alpha/beta or gamma/delta receptor in human atherosclerotic lesions. Am J Pathol. 1993; 142:1927–1937. [PubMed: 8099471]

46. Chambless LE, Zhong MM, Arnett D, Folsom AR, Riley WA, Heiss G. Variability in B-mode ultrasound measurements in the atherosclerosis risk in communities (ARIC) study. Ultrasound Med Biol. 1996; 22:545–554. [PubMed: 8865551]

47. Bots ML, Hoes AW, Hofman A, Witteman JC, Grobbee DE. Cross-sectionally assessed carotid intima-media thickness relates to long-term risk of stroke, coronary heart disease and death as estimated by available risk functions. J Intern Med. 1999; 245:269–276. [PubMed: 10205589]

48. Chambless LE, Folsom AR, Clegg LX, Sharrett AR, Shahar E, Nieto FJ, et al. Carotid wall thickness is predictive of incident clinical stroke: the Atherosclerosis Risk in Communities (ARIC) study. Am J Epidemiol. 2000; 151:478–487. [PubMed: 10707916]

Appendix

Sites and Investigators

University Hospitals of Cleveland (Barbara Gripshover, MD); Tufts University (Abby Shevitz, MD (deceased) and Christine Wanke, MD); Stanford University (Andrew Zolopa, MD); University of Alabama at Birmingham (Michael Saag, MD); John Hopkins University (Joseph Cofrancesco, MD and Adrian Dobs, MD); University of Colorado Heath Sciences Center (Lisa Kosmiski, MD and Constance Benson, MD); University of North Carolina at Chapel Hill (David Wohl, MD and Charles van der Horst, MD*); University of California at San Diego (Daniel Lee, MD and W. Christopher Mathews, MD*); Washington University (E. Turner Overton, MD and William Powderly, MD); VA Medical Center, Atlanta (David

Rimland, MD); University of California at Los Angeles (Judith Currier, MD); VA Medical Center, New York (Michael Simberkoff, MD); VA Medical Center, Washington DC (Cynthia Gibert, MD); St Luke's-Roosevelt Hospital Center (Donald Kotler, MD and Ellen Engelson, PhD); Kaiser Permanente, Oakland (Stephen Sidney, MD); University of Alabama at Birmingham (Cora E. Lewis, MD).

FRAM 2 Data Coordinating Center

University of Washington, Seattle (Richard A. Kronmal, PhD, Mary Louise Biggs, PhD, J. A. Christopher Delaney, Ph.D., and John Pearce).

Image Reading Centers

St Luke's-Roosevelt Hospital Center: (Steven Heymsfield, MD, Jack Wang, MS and Mark Punyanitya). Tufts New England Medical Center, Boston: (Daniel H. O'Leary, MD, Joseph Polak, MD, Anita P. Harrington).

Office of the Principal Investigator

University of California, San Francisco, Veterans Affairs Medical Center and the Northern California Institute for Research and Development: (Carl Grunfeld, MD, PhD, Phyllis Tien, MD, Peter Bacchetti, PhD, Michael Shlipak, MD, Rebecca Scherzer, PhD, Mae Pang, RN, MSN, Heather Southwell, MS, RD)

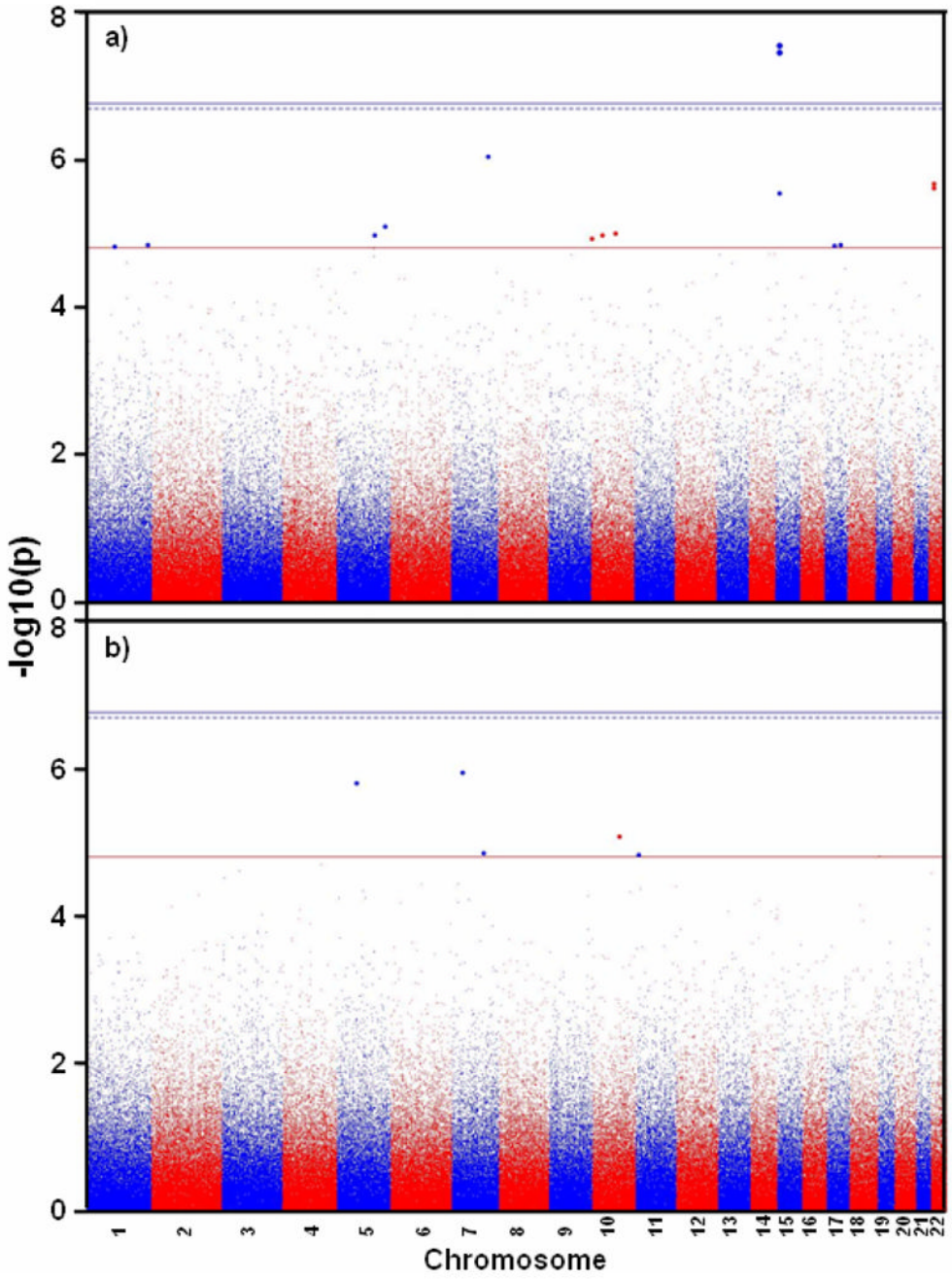

Figure 1.

Manhattan plot showing the genome wide association p-values of single nucleotide polymorphism (SNPs) with a) common carotid IMT (cIMT) and b) internal cIMT. The dark blue solid line indicates the *Bonferroni* threshold, the dotted blue line indicates the threshold based on the effective number of independent tests and the red solid line indicated the threshold at $1.5*10^{-5}$.

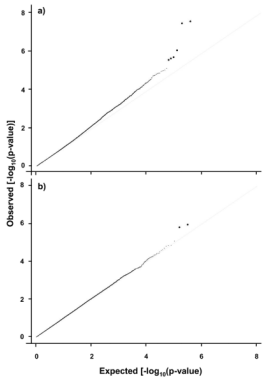

Figure 2.
Q-Q plot of observed versus expected p-values of association with a) common carotid IMT (cIMT) and b) internal cIMT.

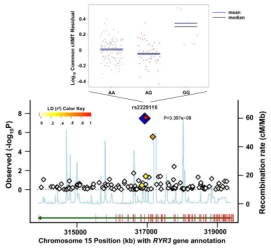

Figure 3.

A comprehensive distribution of 122 informative SNPs from the Illumina humanCNV370-quad beadchip in the *RYR3* gene spanning from 31,390,469 to 31,945,595 bp genomic location in chromosome 15 and the −log (p-values) (left y-axis) of genomic association with common carotid IMT (cIMT). The blue colored SNP is the functional SNP (*rs2229116*) that was associated at the genomic significance level after *Bonferroni* adjustment. The colors of the other SNPs indicate the linkage disequilibrium (LD) (r^2) in relation to *rs2229116*. The right y-axis is the recombination rate shown in blue graphical lines to define recombination hotspots within the *RYR3* gene. The dotspot graph at the top represents the $\log_{10}(p)$ values of common cIMT residual (after adjusting for age, HAART duration and first principal component) along with mean and median by genotype for *rs2229116*.

Table 1

SNPs significantly associated with common and internal carotid intima-medial thickness (cIMT).

SNP	Alleles[‡] MAF	Position	Chr	Related Genes	Location[¥]	Genomic p-value	cIMT [95%CI] (mm)/n by genotype[§]	Genotype p-value[¶]
Common cIMT								
rs1160318	C/a 0.24	95476032	1	*RWDD3*	Intron*	1.50×10^{-5}	0.74 [0.71–0.76]/10 0.83 [0.79–0.87]/63 0.88 [0.85–0.92]/99	0.00017 0.04 -
rs12046077	T/c 0.30	235511722	1	*RYR2*	Intron*	1.40×10^{-5}	0.98 [0.90–1.07]/17 0.87 [0.84–0.91]/70 0.81 [0.79–0.84]/84	0.0002 0.006 -
rs11241998	C/t 0.12	128807258	5	*ADAMTS19*	16,744 bb upstream	1.05×10^{-5}	1.13 [0.90–1.40]/4 0.90 [0.85–0.97]/35 0.84 [0.81–0.86]/133	0.0002 0.04 -
rs958994	A/g 0.27	164996462	5	-	-†	7.97×10^{-6}	1.04 [0.89–1.22]/11 0.87 [0.83–0.90]/69 0.82 [0.80–0.85]/90	0.00002 0.39 -
rs17691394	A/g 0.20	126111827	7	*GRM8*	Intron*	8.81×10^{-7}	1.32 [1.03–1.69]/4 0.86 [0.82–0.89]/59 0.84 [0.81–0.87]/108	0.00003 0.98 -
rs10508211	G/a 0.16	1553135	10	*ADARB2*	Intron*	1.15×10^{-5}	1.50/1 0.92 [0.87–0.97]/52 0.82 [0.80–0.84]/119	0.007 0.001 -
rs274304	G/a 0.31	25287012	10	*PRTFDC1*	5473 bp downstream	1.03×10^{-5}	0.99 [0.89–1.10]/23 0.83 [0.79–0.86]/65 0.84 [0.82–0.87]/83	0.002 0.12 -
rs7079524	A/g 0.18	72739498	10	*SLC29A3*	9518 bp upstream	9.70×10^{-6}	0.70 [0.65–0.77]/5 0.83 [0.79–0.87]/52 0.87 [0.84–0.90]/115	0.00003 0.72 -
rs2229116	**A/g 0.18**	**31692702**	**15**	***RYR3***	**Missense***	$\mathbf{3.40\times10^{-8}}$	**1.15 [0.95–1.38]/8 0.83 [0.78–0.87]/48 0.85 [0.82–0.87]/115**	**0.000002 0.23 -**
rs7177922	**G/a 0.18**	**31695911**	**15**	***RYR3***	**Intron***	$\mathbf{2.74\times10^{-8}}$	**1.19 [0.97–[1.45]/7 0.83 [0.78–0.87]/50 0.85 [0.82–0.87]/115**	**0.000002 0.21 -**
rs2291734	G/a 0.15	31715792	15	*RYR3*	Intron*	2.82×10^{-6}	1.19 [0.91–1.37]/8 0.82 [0.77–0.88]/35 0.85 [0.83–0.87]/126	0.0001 0.11 -
rs10512468	G/a 0.33	30625065	17	*SLFN5*	6191 bp downstream†	1.44×10^{-5}	0.82 [0.76–0.88]/15 0.90 [0.87–0.94]/82 0.81 [0.78–0.84]/74	0.97 0.0002 -
rs4793874	C/a 0.11	53009565	17	*MSI2*	Intron*	1.38×10^{-5}	1.39 [1.08–1.78]/3 0.80 [0.75–0.84]/32 0.86 [0.84–0.89]/136	0.0006 0.07 -

SNP	Alleles‡ MAF	Position	Chr	Related Genes	Location¥	Genomic p-value	cIMT [95%CI] (mm)/n by genotype§	Genotype p-value¶
rs13053817	C/a 0.18	28177722	22	*RFPL1, AP1B1, THOC5, NF2*	Intragenic within 250 kb	2.04×10^{-6}	1.21 [0.95–1.54]/5 0.86 [0.82–0.91]/15 0.84 [0.81–0.86]/115	0.000006 0.99 -
rs5763254	T/c 0.19	28193152	22	*RFPL1, AP1B1, THOC5, NF2*	Intragenic within 250 kb	2.37×10^{-6}	1.21 [0.95–1.54]/5 0.86 [0.81–0.90]/52 0.84 [0.81–0.87]/111	0.000007 0.87 -
Internal cIMT								
rs1697137	T/c 0.36	66487931	5	*MAST4*	Intron*	1.53×10^{-6}	0.96 [0.85–1.08]/24 1.32 [1.22–1.44]/76 1.00 [0.93–1.08]/69	0.98 0.00001 -
rs17151904	G/a 0.20	25574934	7	-	-†	1.11×10^{-6}	1.16 [0.91–1.47]/9 0.93 [0.85–1.02]/49 1.23 [1.14–1.31]/106	0.80 0.000003 -
rs996642	G/a 0.21	105236581	7	*ATXN7L1*	Intron*	1.37×10^{-5}	1.93 [1.55–2.40]/7 1.24 [1.12–1.36]/56 1.04 [0.97–1.11]/105	0.0002 0.05 -
rs588517	G/a 0.15	3143226	10	-	-†	8.11×10^{-6}	2.36 [1.91–2.91]/4 1.23 [1.10–1.38]/43 1.07 [1.01–1.13]/121	0.0001 0.06 -
rs10500651	T/g 0.31	5530156	11	*OR51B5, OR52B6, OR52H1, UBQLN3*	Intragenic within 250 kb	1.44×10^{-5}	1.04 [0.88–1.23]/16 1.26 [1.15–1.38]/73 1.04 [0.97–1.20]/80	0.40 0.00003 -

‡ Second allele is the minor allele;

¥ gene location or distance from gene

* SNP lies in gene,

† not near any genes within 250 kb;

§ in the order of minor allele homozygote, heterozygote and, major allele homozygote;

¶ p-values based on the model comparing residuals of log IMT by genotype (major allele homozygote as reference) with adjustment for age, time duration of HAART and first PCA; all SNPs in HWE p-value>0.001